The anatomy of a flash flood in the Hartbeespoort catchment

JR Hely-Hutchinson* and EH Schumann
University of Port Elizabeth, PO Box 1600, Port Elizabeth 6000

Abstract

As in many other semi-arid regions, rainfall in northern South Africa is erratic in both space and time. In response to such rainfall, runoff in the Hartbeespoort catchment tends to be flashy, particularly runoff arising from rain falling on paved surfaces in the northern suburbs of Johannesburg.

A specific flash flood was monitored from the originating storm down to the dissipation of the underflow in the lake. The storm was fairly typical of the region. Owing to low pondage in the channel, the velocities of the surge and current were almost equal and the hydrograph at the lower end of the channel could be derived by a simple model from those higher up. Two distinct silt loads were generated by the flood, the first probably containing larger particles eroded from around the channel and the second containing smaller particles eroded from the ground upon which the rain had fallen. The second silt load appeared to aggregate a large proportion of the chemicals dissolved in the river and to lead to a density current which produced anomalies in the normal current and temperature profiles. The underflowing flood-water displaced the water resident in the drowned river channel well down into the lake, but entrained sufficient upper-level water during its passage to warm it to a temperature which prevented it from reaching the deepest parts of the lake.

Introduction

Rain tends to fall erratically over arid and semi-arid regions (Christian and Parsons, 1959; Macmahon, 1979), including the northern part of South Africa. In winter, the region lies in the dry zone between the tropical convection zone and the temperate/cyclonic zone, while in summer it lies within the tropical convection zone itself. Rain in summer falls predominantly in the form of scattered thunderstorms, generally lasting around an hour, travelling in a swathe less than 20 km wide and often persisting, at any particular spot, for less than 15 min (Alexander, undated). Because of the strength and scattered nature of the rainfall, the resulting river flow tends to be flashy. Since rain falls mainly in late afternoon (Preston Whyte and Tyson, 1988), as much as 16 h may elapse before the cold runoff is heated significantly by radiation. Thus river water debouching into lakes is expected to dive under warmer resident water (Hutchinson, 1957).

Lake Hartbeespoort is situated in the highveld region of northern South Africa, some 250 km south of the tropic of Capricorn (Fig. 1A). At full supply, its surface lies 1 162 m above mean sea level (m a.m.s.l.). The lake forms the sink to a catchment (Fig. 1A) shaped like an irregular semi-circle. Mean annual rainfall over the catchment is estimated by Pitman (1986) to be 685 mm per year. Streams originating from rainfall flow from the southern perimeter to the terminal impoundment at the centre of the semi-circle in the north, subject to a straight-line gradient of approximately 1:70.

The mean annual runoff from the total catchment is estimated by Pitman (1986) to be 163 x 10^6 m^3. The section of the catchment drained by the Magalies River, although large in area, yields less than 10% of this (Robarts et al., 1982), since the main volume of precipitation over this section appears to be transpired by the vegetation covering it (Van Riet, 1987). The subcatchment over which most runoff occurs includes the headwaters of the Jukskei River and Braamfontein Spruit, and covers an area of some 500 km^2. This subcatchment contains a large proportion of the 12% urban cover of the total catchment, within which the pavements (61 km^2 in 1984, according to Pitman, 1986) roofs and culverts are expected to give rise to rapid and high runoff (NIWR, 1985).

* To whom all correspondence should be addressed.
☎ (0291) 43258; fax (0291) 42384; e-mail hhmodels@intekom.co.za
Present address: Moolmanshof, 217 Voortrek St, Swellendam 6740.
Received 17 July 1996; accepted in revised form 1 April 1997.

The lake capacity, at full supply level, is 195 x 10^6 m^3, under a surface area of around 20.3 km^2, giving a mean depth of 9.5 m. The local geology determines its cruciform shape, with the main body stretching from east to west and confined between two east-west ridges. The gorge in which the dam-wall lies follows the same NE-SW fault as the Crocodile River (Fig. 1B).

In order to examine the effects of influx on the lake, the development of an isolated flash flood in a river channel and its debouchement is described. This medium-severity flood occurred in March 1984, after a three-week rainless period, and during a three-year drought.

Hydrology

Intensities of rainstorms which give rise to floods can be estimated in three dimensions with weather radar, subject to interpretation of the effects of factors such as temperature inversions, water vapour pressure gradients and ground clutter. They can alternatively by assessed with rain gauges, subject to difficulties involved in building three-dimensional pictures from often unevenly distributed point-sources in uneven terrain. They can thirdly be assessed in integrated form with flow meters in the runoff channels, subject to effects of factors such as capture, transpiration and seepage (Mimikou and Baltas, 1996).

The time of concentration of runoff at the lowest point in the catchment under a rainstorm can be calculated in terms of the Bransby-Williams equation (Alexander, undated):

$$t_c = k_b(L_s^{1.2} /(H_s^{0.2}A_c^{0.1})) \qquad (1)$$

where:

- t_c = the time it takes for precipitation falling on the hydraulically most remote point of the rainstorm to reach the lowest point
- L_s = length of main river or reach
- H_s = height difference from remote point to outlet
- A_c = area of catchment
- k_b = constant.

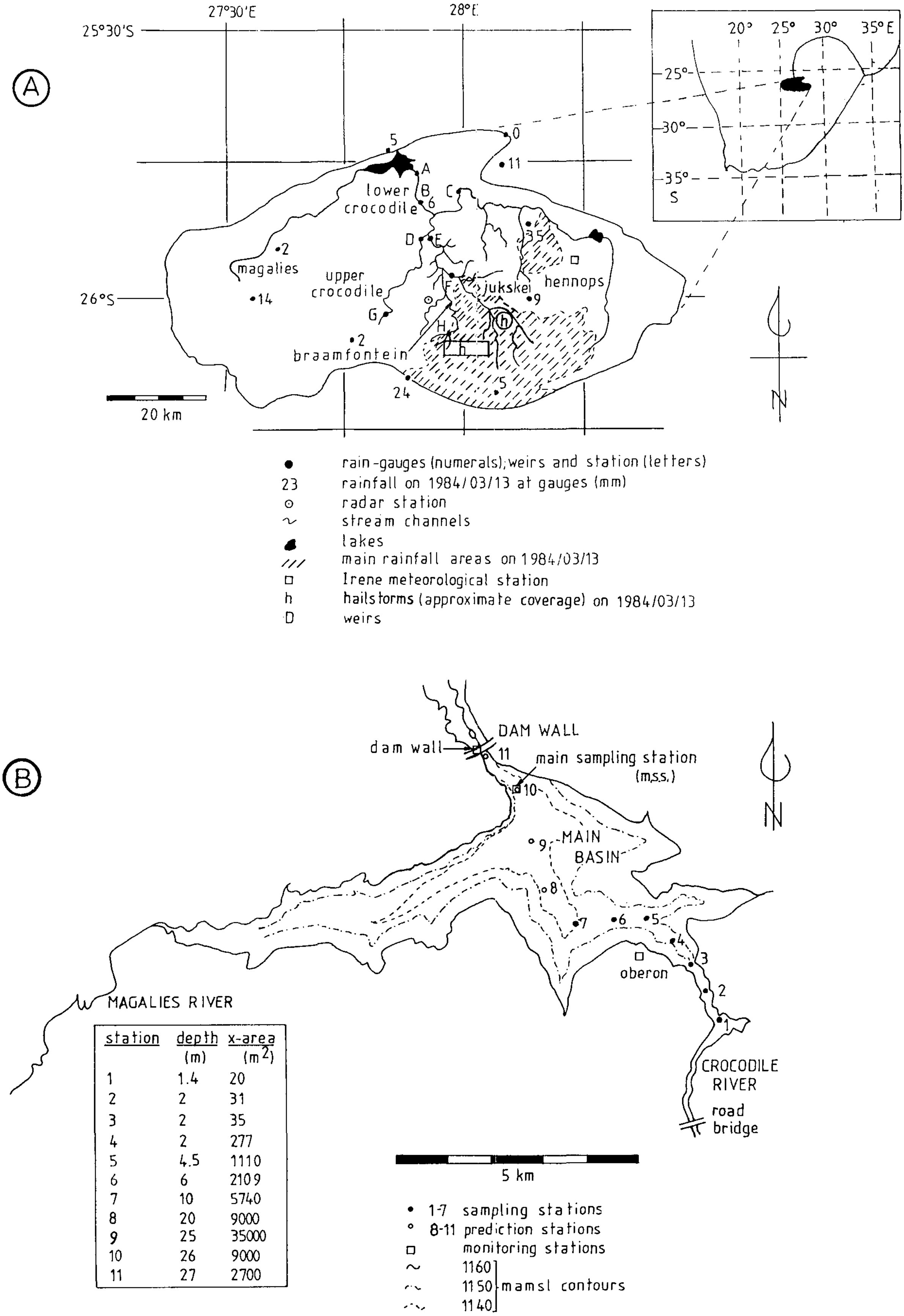

station	depth (m)	x-area (m^2)
1	1.4	20
2	2	31
3	2	35
4	2	277
5	4.5	1110
6	6	2109
7	10	5740
8	20	9000
9	25	35000
10	26	9000
11	27	2700

Figure 1

A *- Hartbeespoort catchment, showing locations of main tributaries, rain gauges (together with precipitation on 1984/03/13) and principal weirs, and location of the catchment in Southern Africa.*

B *- Shoreline and bottom contours of Lake Hartbeespoort showing sampling, prediction and monitoring stations, together with depth and cross-sectional area at each lake station.*

The velocity of the flood front can be calculated in terms of the Manning equation, one of the simplest of many equations relating capacity, hydraulic gradients, bottom roughness and channel size (Chow, 1964).

$$U_w = k_m R_s^{0.67} S_s^{0.5} k_{rf}^{-1} \quad (2)$$

where

R_s = hydraulic radius of the channel (area of cross-section divided by bed perimeter)
S_s = slope
k_{rf} = roughness factor
k_m = constant of proportionality.

Since plan locations, elevations and times of arrival of the leading edge of the flood are known in respect of Weirs F, E and B (Fig. 1A), speeds and gradients between them can be calculated directly. Assuming constant channel roughness and depth, the front velocities and arrival times of a flood wave down a reach where no measurements were taken, can thus be calculated from data gathered in others. Such calculations are applied to all four of the tributaries, namely the Crocodile, Braamfontein, Jukskei and Hennops Rivers (Fig. 1A).

In order to improve understanding of the river hydrology, discharge over Weir B is predicted from those over other weirs by a mathematical model. The choice of models is wide. The rainfall/runoff model described by Pitman and Basson (1979) predicts runoff accurately over daily integrations but not accurately enough for this study on an hourly basis. The persistent sharpness of the leading edge of the monitored flood tallies badly with models such as Kulandaiswami's (Chow, 1964), which consist of networks of first-order lags, and a more basic approach is needed. Direct delay and quantity models are used in practice.

It will be shown that the match of the model output to the data can be improved if the model includes terms relating to storage to, and release from, stilling ponds. It will also be shown that such terms suggest the existence of either additional delays in certain sections of the channel and/or residence as groundwater (see Pitman and Basson, 1979), and/or contributions from unmonitored tributaries.

Properties of water

The temperature of water flowing towards a lake is affected by the surface energy balance (Fischer et al., 1979), which depends in turn on the period of travel and on the nature and environment of the channel down which the water flows. For instance water which travels mainly at night will tend to remain cooler than that which travels mainly by day. Also Ward (1985) states that:

- *in the shaded headwaters of a tropical river, water temperatures tend to remain close to mean air temperature;*
- *where the canopy of vegetation is more open, water temperatures may approach or even exceed air temperatures;*
- *hail can reduce water temperatures by as much as 10°C, and quite suddenly.*

Variability of runoff in catchments such as Hartbeespoort may significantly affect three processes important in the lake, namely sedimentation, aggregation and oxygenation.

Sedimentation covers erosion, transport and deposition of particles by flowing water. The properties of the above processes are summarised by Smith (1975). The density of the water itself is influenced by the concentration and size distribution of the particles. In flowing water where this influence is significant, currents which flow at the level consistent with such densities are known as turbidity currents, which can involve particles of silt and clay (Chikita, 1989).

The nature and concentrations of suspended particles also affect concentrations of chemicals (nutrients) which occur at harmful levels in many eutrophied impoundments (Carmichael, 1981). Chemicals which give rise to eutrophication are often associated with effluents discharged by industrial plants into influent rivers (Barica and Muir, 1980), while other chemicals are associated with irrigation. Sources of chemicals are, in many rivers, so widely distributed that it has sometimes been impossible to locate the sources in order to prevent harmful chemicals from being injected. It is thus worthwhile to understand the behaviour of chemicals within rivers and lakes with a view to controlling them in transit.

Knowledge of the interactions between chemicals and sediments in natural waters has not, up to now, been co-ordinated. Chapra (1980) believed that a large proportion of introduced chemicals, such as phosphorus and organic toxins, are adsorbed onto river and lake sediments, though the total mechanism of adsorption is not yet fully understood. However, Stumm and Morgan (1970) have claimed that aggregation of colloids is of great importance in the transport and distribution of matter in natural waters. Viner (1984) has confirmed that suspended loads in flowing waters could transport large amounts of phosphate. He has singled out clay particles for particular mention. After an extensive literature search, Woodard et al. (1981) concluded that most metals (including heavy metals) are found adsorbed onto suspended material. The same tendency was noted by Grobler et al. (1987) in the Vaal River.

Lakes which act as sinks to the influent water are stratified into a range of density levels, particularly in summer (Imberger and Patterson, 1990) . Since the chemical content of most freshwaters, including that of Hartbeespoort, is too small to affect density significantly, density is defined effectively by temperature alone. Where influx is colder than water at the surface of a lake, it dives underneath the surface along a line known as the plunge point, and settles within the lake at approximately the level at which the water temperature equals its own (Hutchinson, 1957; Imberger, 1982). Where inflow is cooler than the entire profile of the standing water, it tends to dive to the bottom. In catchments where inflow is persistently colder than the terminating lake, the diving stream may be an important agent in maintaining a temperature differential across the vertical column. However, even very cold underflow entrains warmer water from the upper strata as it travels down a drowned river valley. Thus, even if the influent water is initially colder than any of the resident lake water, it may not remain cold enough to reach the deepest part of the lake (Imberger and Patterson, 1990).

Explanations of methods used for calculating underflow speeds and temperatures in this paper are provided by Hebbert et al. (1979), Akiyama and Stefan (1984) and Imberger and Patterson (1990).

Data and methods

Rainfall distributions and intensities giving rise to the flood were derived mainly from radar patterns at the meteorological station indicated in Fig. 1A supplied by the Atmospheric Physics Division of the National Research Laboratory (NPRL), now part of Environmentek, CSIR, according to methods described by Held

(1988). Confirmation was received from rain-gauge readings, integrated over daily periods, supplied by the Weather Bureau, according to methods formulated in 1987. Due to their scattered locations, the relevances of rain-gauge readings to the pattern of river currents was regarded as low, but it will be seen below that the sparse readings were in fact confirmed by the hydrology.

Hailstorm records were contributed by the NPRL. The records are derived from observations by volunteer hail watchers. The hailstorm statistics provided by the hail watchers include station co-ordinates, date, starting time, duration, stone size distribution, correlation with rain and spacing between stones. Estimates are also made of areas covered by two hailstorms which could have affected the temperature of the monitored flood.

Records of inflow to Lake Hartbeespoort were measured in terms of water levels over weirs by the DWAF. Records of temperature and conductivity at Weir B (Fig. 1A) over 11 d including the monitored flood were provided at hourly intervals. Temperatures and conductivities were measured to an accuracy of 1°C and 4 $mS \cdot m^{-1}$ respectively.

Air temperature was measured at Oberon (Fig. 1B) on analog charts by the Department of Water Affairs and Forestry (DWAF), to an accuracy of 0.1°C. Short-wave radiation was also measured at Oberon on analog charts by the DWAF with a variation of 1.5% due to temperature and with 1% selective attenuation over the band from 315 to 2 200 nm (Bosman, 1983). Both data vectors were used at 1 h intervals.

At the main sampling station in the lake (Fig. 1B), water temperatures were measured, at 1 m depth intervals, with a Cole Parmer thermistor bridge, to a resolution of 0.01°C, and conductivities with a W.T.W. model LF 56 to an accuracy of 0.1%.

A variety of hand measurements detailed below was carried out at Stations 1 to 7 in the debouchement (Fig. 1B), in order to amplify knowledge of the behaviour of the flood in the debouchement of the lower Crocodile River into Lake Hartbeespoort. Readings were taken at the following nominal depths below the surface: 0, 0.5, 1, 1.5, 2, 2.5, 3, 3.5, 4, 5, 6, 7 and 8 m. Water speeds were measured, at roughly the centre of the channel, with an Ott type propeller, averaged over a minute or so, with a threshold of 0.05 $m \cdot s^{-1}$. As they were measured from an anchored boat, accuracies are also assessed as ± 0.05 $m \cdot s^{-1}$. Temperature and conductivity were measured with the same equipment as at the main sampling station. Dissolved solids concentrations were estimated in terms of conductivities. Following the advice and general methods of Smith (undated), all conductivity readings were standardised (C_{25}) to conductivities at 25°C. Taras et al. (1971) stated that total filterable residue is roughly proportional to conductivity. Solute transport rate is therefore taken as proportional to the product of discharge and dilution.

Following the experience of Grobler et al. (1981), turbidity is used as an indicator of suspensoid load. Turbidity was measured with a Hach Turbidimeter model 16800, accuracy 2 nephelometric turbidity units (NTU), which registered only up to 100 NTU. Samples with higher turbidities were diluted and the readings multiplied pro rata (HACH, undated).

In order to cover the storm event as well as the entry of the water into the debouchement, the elapsed times of all the 4-hourly measurements are referred to a datum at 00:00 on 1984/03/13. In order to leave time for equipment preparation, boat servicing and operator changing, and to process the conductivity and turbidity readings, complete sets of readings at all stations in the debouchement were taken at nominally 4 h intervals. However, it took about 1.5 h to complete each set of readings at all the stations, and to this extent the nominal times are approximate.

In order to simplify the presentation of the total matrix of hand measurements, all elements in Figs. 3B, 4, 5 and 6 are referred to nominal times. Since not all the readings were taken at all nominal depths, missing elements are filled in by duplicating values from the elements directly above. There are two exceptions to this procedure. Firstly, missing current speeds are tapered linearly to zero from the lowest location at which readings were available to the bottom of the channel and secondly, missing temperatures in the underflow stratum are filled in in terms of underflow calculations.

At Station 5 (Fig. 1B), additional temperature measurments with an Anderaa automatic profiler, resolution 0.03°C, at 15 min time intervals and 0.4 m depth intervals.

The debouchement readings were taken at intervals downstream from the furthest point upstream to which the boat could be driven (Station 1 in Fig. 1B). Thus the water level was the same as that of the lake. The rise in water level during the flood is calculated in terms of contemporary lake data provided by the DWAF. It will be shown that the change in water level before and during the flood was small enough to be neglected.

F-ratios (Hunter, 1968), that is ratios of differences between data vectors and the mean to deviations between data vectors, are used as criteria of fit where it is necessary to compare deviations from data with spreads of data. Where one of the vectors is a model output, degrees of freedom and probabilities of null hypotheses can be calculated, that is the chance that the model output should equal the mean rather than the data.

Events in the catchment

The type of storm was selected in collaboration with the NPRL, with the aim of predicting a typical flood. To include the effect of the paved surfaces, such a storm had to break over Johannesburg, some 50 km from the lake. It was estimated that an interval of nearly 12 h would elapse while the flood wave travelled down the tributaries before reaching the lake, during which interval monitoring equipment could be deployed at the debouchement into the lake. To remove the effects of antecedent rainfall (Alexander, 1990) and thus make it easier to relate physical effects in the lake uniquely to the monitored flood, it was hoped that the flood would be isolated from previous and susbsequent floods.

After several weeks of dry weather, a heavy rainstorm was detected over northern Johannesburg at 15:00 on 1984/03/13 by the CSIR weather radar (Fig. 1A). Initial analysis of the readings indicated that the storm would develop in a manner typical of the region. Monitoring equipment was deployed at the lake and the ensuing flood was traced in all its phases, from the weather pattern and the originating rainstorm through surface runoff and discharge down the confluent channels into the debouchement and under the lake itself.

Held (1988) has confirmed that the effect of this storm on the subcatchment was not unusual for the region. The approximate area of heavy rainfall estimated from radar which gave rise to the flood is related to river channels in Fig. 1A, in which are also plotted rainfall readings integrated over 1984/03/13. Held's data identify two main wetted areas relevant to this study, namely those over the northern suburbs of Johannesburg and over the Hennops River.

The leading edge of the section of the storm over Johannesburg progressed about 20 km in a northerly direction within approxi-

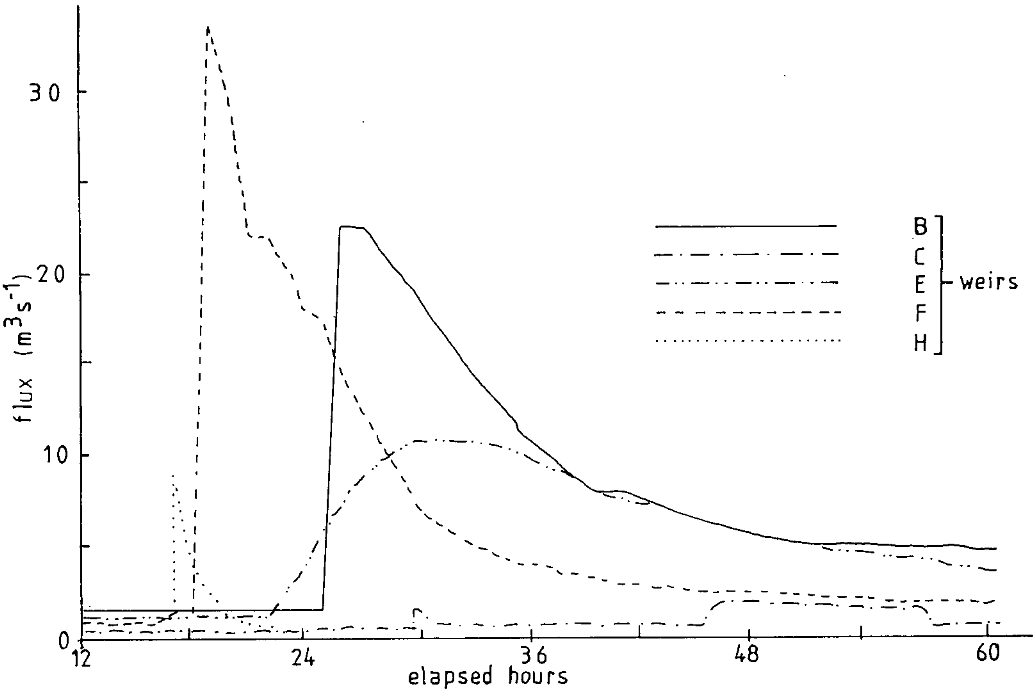

Figure 2
Hydrographs measured on 1984/03/13-15 at Weirs B; C; E; F and H in Hartbeespoort catchment (Fig. 1A). Time origin at 00:00 on 1983/03/13.

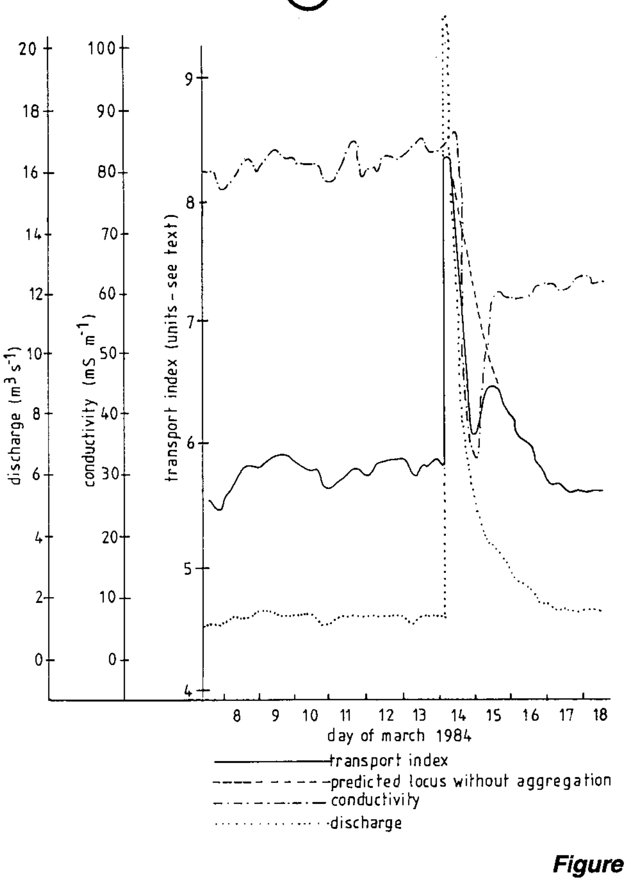

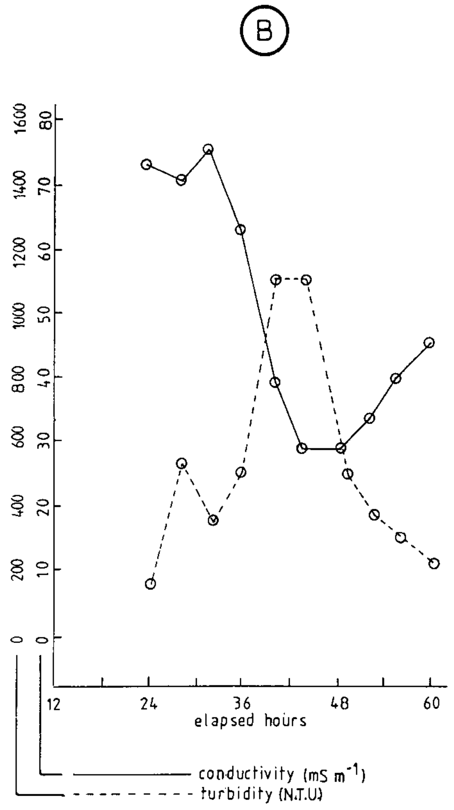

Figure 3
A *Conductivity corrected for temperature and natural logarithms of an index proportional to solute transport at Weir B in Hartbeespoort catchment (Fig. 1A) over 1984/03/08-18.*
B *Conductivity and turbidity at point A in Hartbeespoort catchment (Fig. 1A). Time origin at 00:00 on 1983/03/13.*

mately 1 h (Held, 1988). Resolving this progress to the NNW orientation of the river channel yields a velocity of about 18 km·h^{-1}. However, the channel is far from straight. The ratio between channel length and line of sight may be as high as 1.4, in which case the velocity of the leading edge of the storm down the river bed would have been 25 km·h^{-1} (8 m·s^{-1}).

Rain-gauge readings and gaps between stations (Fig. 1A) are consistent with a swathe of precipitation around 10 km wide. A mean precipitation of 10 mm during the hour over an area of 500 km^2 is inferred from Held (1988), yielding a total precipitation of 5 x10^5 m^3. The storm pattern is confirmed by the spatial distribution (Fig. 1A) of the patterns of discharge over the weirs (Fig. 2). The isolation of the flood is demonstrated by the hydrograph at Weir B plotted over 11 d in Fig. 3A. Of the estimated 5 x 10^6 m^3 water precipitated, about 10^6 m^3 entered the river within 2 d, indicating a runoff-to-rainfall ratio of 0.2, which closely approximates that derived by Kovacs (1978) investigating a storm in the catchment, for discharge over Weir B, and near the mean (0.3) of those he derived in respect of Weirs C, D and E. In view of the fairly constant subtractions by capture and evapotranspiration in the vegetated sections of the subcatchment, such a higher figure is expected in respect of a larger flood.

The leading edge is unusually sharp compared to those of flood hydrographs in the U.S.A. discussed by Meinzer (1942), Linsley et al. (1949) and Chow (1964). The sharpness is consistent with the direction of expansion of the storm downstream in the direction of the channel, a consequence investigated by Foroud et al. (1984).

Two hailstorms within the area covered by the storm were reported by the NPRL. The first, roughly located near Weir H (Fig. 1A), lasted between 15:00 and 15:40, peaking around 15:25 and including hailstones between 2.5 and 5 cm diameter. The ground was not fully covered by the stones. The leading edge of the hailstorm progressed at 1 km·h^{-1} eastwards for about 10 km in a 3 km broad band along the path shown in Fig. 1A. Preston-Whyte and Tyson (1988) have noted that hailstorms often travel in narrow bands along straight paths. Although the hailstorm progressed at right angles to the leading edge of the main storm, the motion of the leading edge was associated more with expansion than with migration of the entire storm (Held, 1988). The second hailstorm, roughly located some 20 km to the north-east end of the first, included stones 2.5 cm diameter and lasted from about 15:40 to 16:00. Some hail may well have fallen over or near the water-courses and contributed to cooling the runoff.

All hydrographs associated with the storm are shown in Fig. 2. At no other weirs in the subcatchment were large discharges reported during the period. The most significant hydrographs were obtained at Weirs H, F and B. The shapes of the hydrographs confirm Alexander's (1990) claim that rainfall from convectional storms tends to peak at the beginning of the storms. Weir H registered a discharge of 9 m^3.s^{-1} within an hour of the cessation of the storm, after which a total of about 0.1 x 10^6 m^3 water passed over it. Over Weir F flowed a total volume of around 10^6 m^3, beginning with a peak discharge of 34 m^3·s^{-1}, 2 h after the storm had ceased. The leading edge of the flood took a further 7 h to reach Weir B, at which point peak discharge had decreased to 23 m^3·s^{-1}. The total volume remained at around 10^6 m^3. The shape of the hydrograph at E differs from the others, and Keuris (1985) believed that the measuring system was probably faulty, but that the onset of the rise in level was correctly indicated. Of the remaining hydrographs, Weir D is believed to have registered only base flow, the highest reading over the period being 0.16 m^3·s^{-1}. The hydrograph over Weir C confirms the existence of the storm over the Hennops River, with maximum readings of only 1.66 m^3·s^{-1}. According to Held (1988), this is attributed to evapotranspiration from a non-urban area.

In assessing the time of concentration (t_c in Eq. 1) between the storm and Weir F (Fig. 1A), the data are as follows:

A_c = 500 km^2;
L_s = 20 km;
H_s = 200 m;
and t_c is calculated to be 6.5 h.

Reckoned from the mean time-of-day of the storm (15:30 or 15.5 e.h., in other words elapsed hours in Figs. 3 to 6), the time-of-day of concentration at Weir F was 22:00 (15.5 + 6.5 = 22.0 e.h.). Judging from Fig. 2, the leading edge arrived at 19:00 (19.0 e.h.), and the centre of gravity (c.g.) of the flood hydrograph arrived at 04:20 (28.3 e.h.). Since the c.g. of the storm occurred at approximately 16 e.h., the instant of concentration (from t_c) at 22.5 e.h. falls between these limits (19.0 and 28.3 e.h.).

In estimating flow velocities down the catchment in terms of the Manning equation (Eq. 2), the low calculated hydraulic radius (0.3 m) of the river during the drought tallies with visual sightings. The river, even down as far as the road bridge (Fig. 1B), flows around rocks which crop out above the surface. Since the channel is wide in proportion to its depth, the condition for overland flow (Linsley et al., 1949) was satisfied and the radius can be defined by depth alone. The value of the roughness coefficient k_{rf} = 0.05, is equal to that used by Kovacs (1978) as appropriate to the catchment. Thus velocity in the catchment is assumed to be independent of discharge and stage. Referring to Meinzer (1942), the relationship between hydrographs taken at Weirs F and B corresponds more closely to that of those taken in the USA. on the North Platte River between Bridgeport and Lisco than to that of those taken on the Stillwater River between Pleasant Hill and Englewood. This suggests that channels in the analysed sector of the catchment include little pondage. Ratios of calculated squares of flow velocities to gradients between Weirs F and E and E and B tally to within 12% of the mean.

In terms of the discharge model, discharges at Weirs F, C and D are compatible with the balance at Weir B. The main residual is a deficit in estimated base flow both before and after the flood. The r.m.s. (root mean square) deviation between measured and modelled discharges is 0.6 m^3·s^{-1}. Averaged over the 48 h period, this amounts to 10% of the 10^6 m^3 volume of water in the flood. Quantities inserted from Weir H are found to be incompatible with close dynamic balance at Weir B, even if delays are adjusted. It is inferred that discharge down the Braamfontein Spruit, including base flow, was trapped or diverted prior to its arrival at the confluence with the Jukskei River. There has been no direct confirmation of this inference.

To improve the match of the model to the data, particularly around the peak, additional short- and long-term delays are inserted of around 1 and 12 h. The short delay suggests smearing associated with channel roughness. The long delay suggests the existence of small inflows long after the arrival of the main leading edge at Weir B, associated perhaps with rainfall near the upper Crocodile and upper Jukskei Rivers (Fig. 1A). However, as suggested by the poor performance of Weir E, the need for additional delays may be associated partly with inaccuracies in flux measurement. According to Alexander (1990), there is no evidence of interflow in South Africa.

There was a 2 h difference between the 7 h travel time of the leading edge of the flood from Weir F to Weir B and the 9 h travel time of the centre of gravity. This indicates only a 23% difference between the velocities of the front and current in the channel. It appears that, as the Froude no. > 1, the standing water could not adjust to the runoff and was pushed down the channel in front of it as plug flow. The difference between the velocities may, however, be explained by the broadening out of the hydrograph due to pondage in the channel.

Current velocity at Station 1 (Fig. 1B), at the start of the flood, also corresponds closely to velocities in the catchment. This indicates that, at that time (28 e.h.), the plunge point had been driven well into the lake beyond Station 1. This deduction was confirmed by the difficulty of holding the boat on station in the violent current during measurements at nominal e.h. 28 and 32 at Stations 1 to 4. The close approximation between front and current velocities indicates that relatively little water (compared to that in the flood) is stored in the channel during base flow. Assuming a mean depth of 0.3 m, width 4 m and length 50 km, the quantity is 0.06 x 10^6 m^3, which accounts for only 6% of the water in the flood.

Transport of dissolved chemicals by the flood is assessed in terms of discharges and conductivities. The curve of conductivity at Weir B, when corrected for temperature (Fig. 3A), shows no evidence of diurnal effects. Before the arrival of the flood, conductivity was relatively constant with only small random variations. During the flood, it dropped rapidly and rose again, after a limited period, to another fairly constant value. The difference between the values before and after the flood appears to have been associated with the discharge. This is confirmed by values of solute transport before and after the flood, which were similar. This suggests that solutes, possibly from municipal and industrial sources, were released at the same rate before and after the flood and that, during the flood, solutes of different concentration were present in the river.

The time locus of solute transport (Fig. 3A) shows how the brief dip in conductivity interrupts what appears otherwise to be a conventional exponential decay, the shape of which resembles that of the discharge. The reduction in products of conductivity and discharge seems unlikely to have been associated directly with discharge alone since, in that case, the locus of conductivity would have been expected to follow the discharge curve more closely. The numerical evidence suggests that reduction in conductivity was caused by another agency. This might conceivably have been exhaustion of available solutes. However, there is no evidence to support such an idea.

Judging from the literature, a more obvious agency is aggregation of chemicals onto particles, as evidenced by the fact that turbidity (Fig. 3B) rose over approximately the same period that conductivity fell. The calculated stream velocity was around 1 $m \cdot s^{-1}$, which would have been capable of raising consolidated particles of between 0.2 mm and 1.2 mm, or unconsolidated particles up to 12 mm dia. (Smith, 1975). Mineral material within this range of dia. was probably available all along the channel (although no assessment was made of particle sizes in the sample bottles).

The deduction concerning aggregation is complicated by the fact that there are two turbidity peaks measured at Station 1 and illustrated in Fig. 3B. The existence and separation of the two peaks are confirmed by measurements at Stations 2 and 3 (not shown in Fig. 3B), which suggest that the material content in the two peaks was about equal. The peaks are differentiated as follows: The first impulse began to rise at the same time as the leading edge of the flood and ended within about 8 h. Bearing in mind the 4 h intervals between measurements, the initial concentration of suspensoids may have begun to drop at the time of the second measurement (at 28 e.h.). Since the validity of the Manning equation (Eq. 2) is confirmed for the catchment, stream velocity would have been unlikely to depend strongly on discharge, and a second, larger sediment load would probably not have been eroded from the bed of the channel as the flood receded.

The suspended particles in the second peak are thus assumed to have been eroded from the ground upon which the rain fell. Gottschalk (1964) emphasised the small size of sheet erosion products and Rooseboom (undated) shed the following light on particle sizes and concentrations:

> *The sediment which is transported in most Southern African rivers is very fine. Because sediment is carried into rivers mainly when they are in flood and possess large capacities for transporting sediments, local rivers are rarely overloaded with sediments. For this reason it is found that singular relationships between sediment loads and discharges do not exist, as the availability of sediment and not the transporting capacity of the streams is the controlling factor.*

Particles derived from sheet erosion could have probably easily been kept in suspension by rivers with velocities much lower than those in the channels. Such particles would thus have been unlikely to have fallen to the bottom as stream velocity decreased (Smith, 1975). Therefore the second pulse of high turbidity was probably composed of particles covering a wide range of sizes.

Numerically, the reactions of conductivity to turbidity (t_p) are different for the two peaks (Fig. 3B). Grobler et al. (1987) typified such reactions with a reciprocal model. It was found that the reactions from this study could be more closely simulated by a configuration of a linear model different to theirs. Note that a gap from 32 to 40 e.h. has been created between the readings analysed in respect of the first peak and those analysed in respect of the second, in order to avoid confusion between sediments characteristic of the two peaks. The reaction of the first peak, evidenced by readings at 24 and 28 e.h., is expressed as $C_{25} = -0.03t_p + 74$, for which the Fisher statistic is $F_{1,40} = 7.4$, $p_n = 0.0096$, while that of the second, evidenced by readings from 44 to 60 e.h., is expressed as $C_{25} = -0.5t_p + 70$, with $F_{1,112} = 21.8$, $p_n = 0.00001$. Thus, in terms of this model, the probability of the null hypothesis for the second peak is nearly 1 000 times smaller than that for the first. The difference may have been due to differences in distributions of particle size and geological origin. The range of particles eroded from the banks of the channel may have been wider and the particles themselves generally bulkier than those eroded from paved surfaces. Grobler et al. (1987) felt that pollutant concentrations in sediment would usually increase with decreasing particle size.

In order to compare relationships between turbidity and conductivity with data published by Grobler et al. (1987), a reciprocal model similar to theirs is generated for the second series. The refined model is $t_p = (12608/C_{25}) + 184$, $R^2 = 0.04$, p_n =0.04. Comparison with their multiplier (= 1959)indicates that conductivity is 0.1 as sensitive to turbidity as in the lower Vaal River, while comparison with their R^2 (= 0.64), suggests there is a much wider spread of relationships in the lower Crocodile River. These two differences suggest more rapid current in the Hartbeespoort catchment, raising a wider and generally bulkier range of particle sizes from the walls of the channel and from the surrounding surfaces than were still in suspension at the time of measurement in the lower Vaal River. It should be noted that

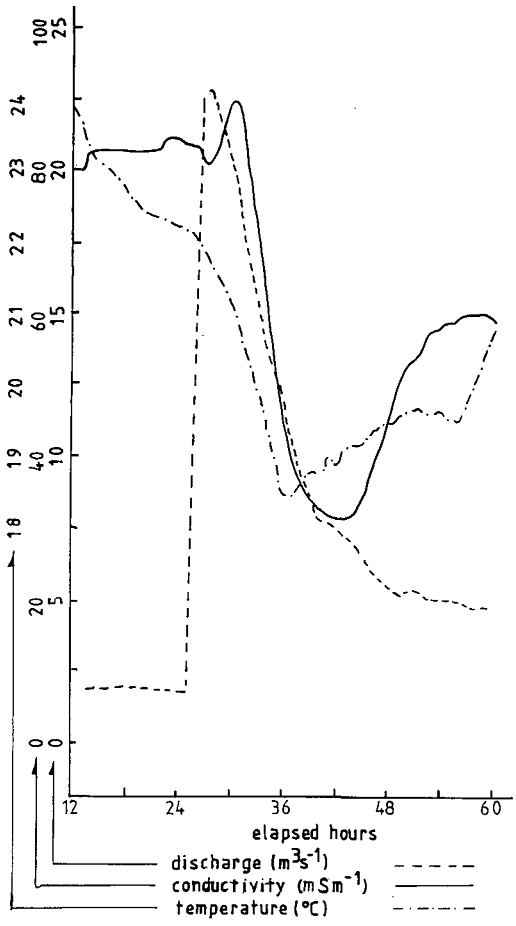

Figure 4
Discharge, temperature and temperature-corrected conductivity at Weir B in Hartbeespoort catchment (Fig. 1A). Time origin at 00:00 on 1983/03/13.

Grobler et al. (1987) regarded changes in turbidity as due solely to flocculation, and thus used turbidity as a dependent variable whereas, in the experiment described above, turbidity is attributed to erosion and is thus an independent variable. Flocculation may also have occurred in the Hartbeespoort catchment and might therefore have influenced the effect.

Temperature in streams reacts quickly to solar radiation and cannot thus be used to identify the movements of hydrols in great detail. However, the steepening of the temperature gradient coinciding with the arrival of the leading edge (Fig. 4) further suggests the near-equality of front and river velocities. Assuming that the onset of the drop in conductivity (at 31 e.h.) corresponded to the arrival of runoff, which is likely to contain a weaker solution of chemicals than the base water, the quantity of water resident in the channel and impoundments prior to the flood can be calculated from the flood flux integrated from the leading edge of the flood (26 e.h.) to 31 e.h. Assuming a mean flux of 18 $m^3 \cdot s^{-1}$, the resident base-water works out at 0.3 x 10^6 m^3. Subtracting 0.06 x 10^6 m^3 for water in the channels, that in the impoundments is approximately 0.24 x 10^6 m^3.

In summary, a quantity balance indicates a physico-chemical relationship between turbidity and conductivity in the river channel. Although no measurements of particle size were taken, nor chemical assessments of aggregation made, numerical evidence suggests that the presence of suspensoids directly affected the level of dissolved chemicals. In proposing this theory, it is not necessary to assume that significant unaggregated solutes entered the river from the runoff area.

In the debouchement

The water in the flood constituted 0.5% of full supply in the lake, or roughly 1% of the supply level during the experiment. Since the surface area of the lake was around 9.6 km^2 at the time, the addition raised the level by only 0.1 m. Such a small rise would not have significantly affected definitions of depth in the debouchement.

TABLE 1
UNDERFLOW TEMPERATURES WITH DELAYS EQUIVALENT TO 8 H BETWEEN STATIONS AND PLUNGE POINT HALFWAY BETWEEN STATIONS 4 AND 5 (FIG. 1B)

e.h. / Station	24	28	32	36	40	44	48	52	56	60
5	23.5	22.5	22.3	23.0	22.9	21.1	20.4	20.0	19.9	20.6
6	24.5	24.5	23.8	23.0	22.8	23.3	23.3	21.9	21.3	21.0
7	24.2	24.2	24.2	24.2	23.7	23.1	22.9	23.4	23.3	22.2
8	24.0	24.0	24.0	24.0	24.0	24.0	23.8	23.5	23.5	23.7
9	23.1	23.1	23.1	23.1	23.1	23.1	23.1	23.1	23.1	22.9
10	22.4	22.4	22.4	22.4	22.4	22.4	22.4	22.4	22.4	22.4
11	22.3	22.3	22.3	22.3	22.3	22.3	22.3	22.3	22.3	22.3

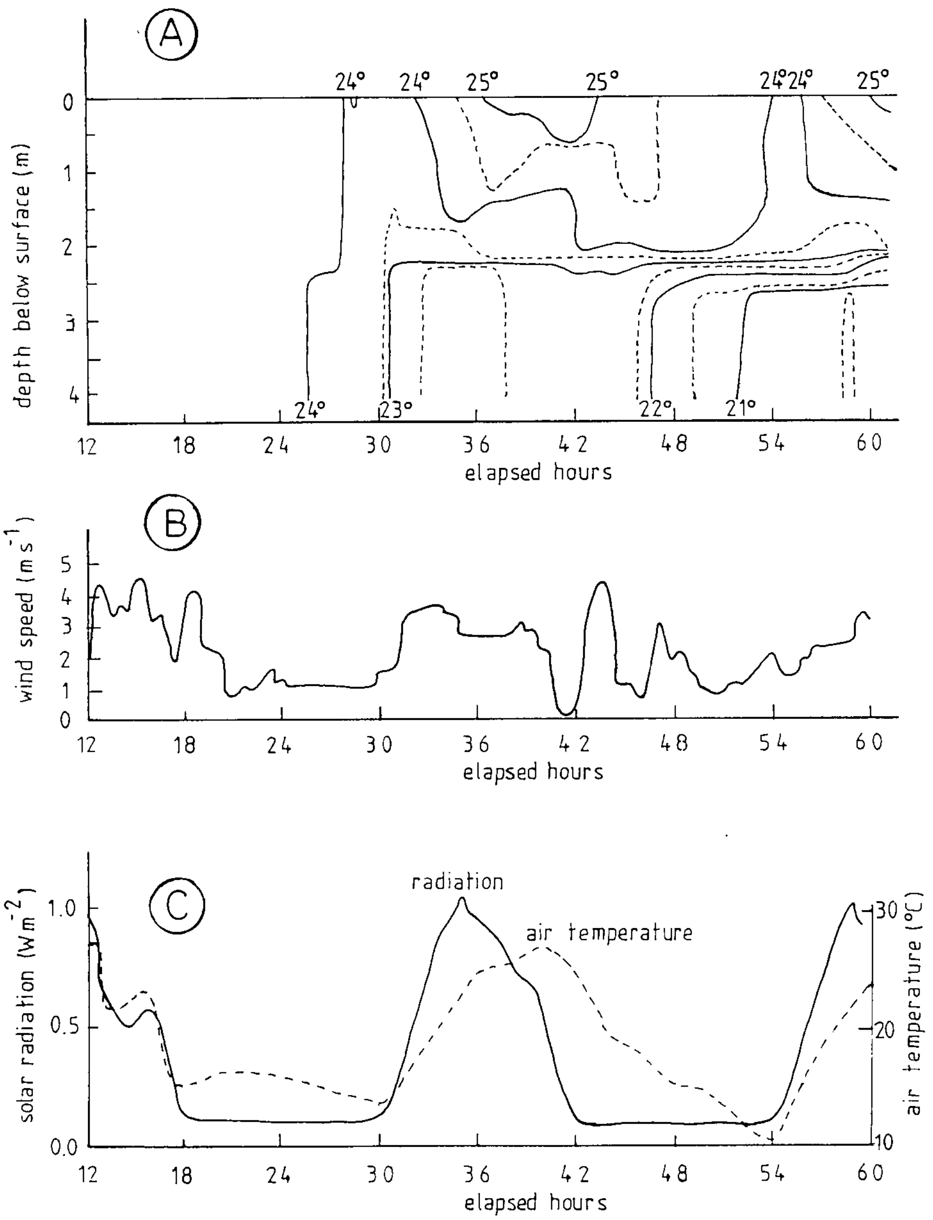

Figure 5
***A** Temperature profile at sampling Station 5 in the debouchement of the Crocodile River into Lake Hartbeespoort (Fig. 1B), on the same time-axis as*
***B** wind-speeds and*
***C** solar radiation and air temperature measured at Oberon in Hartbeespoort catchment (Fig. 1A), during the flood of 1984/03/13-15. Time origin at 00:00 on 1983/03/13.*

again on 1984/03/15. From e.h. 30 onwards, the underflow maintained its integrity from the rest of the profile, falling to near 20°C at Station 5, and18°C further up the channel.

Underflow temperatures calculated according to Hebbert et al. (1979), Akiyama and Stefan (1984) and Imberger and Patterson (1990) are displayed in Table 1. Temperatures below and to the left of the rectangular line are those of the bottom of the standing water before the underflow arrived. Underflow temperatures remained colder than the standing bottom temperatures until the underflow reached location 9 at e.h. 52, around which time and place the underflow is estimated to have flowed horizontally into the lake, because there are no temperature differences at that level.

Inter-relationships between events in the debouchement are illustrated in Fig. 6.

At 00:00 on 84/03/14 (e.h. 24), inflow consisted entirely of baseflow which was imperceptible beyond Station 1. Owing to the low flux, the constant input of dissolved solids loaded the river heavily; a much higher loading than the lake-mean, which included contributions from floods. The inflow temperature was lower than that in the lake, as the inflowing rivers are more sheltered than the lake. The winds associated with the storm had mixed the water through the column at each station. Turbidity was considerably higher than that in the lake, as silt would tend to remain in suspension before settling in the relatively static water of the main basin.

At 04:00 on 1984/03/14 (e.h. 28), the flood-peak passed Stations 1-4. Although turbidity rose between Stations 1 and 3, aggregation probably remained low and conductivity remained high because, it is believed, of the large particles in the first silt load.

The combined effects of wind, radiation and underflow at Station 5 in the debouchement (Fig. 1B) are assessed with reference to Fig. 5. The radiation pattern (Fig. 5C) was modified during the storm. The wind (Fig. 5B) rose to 4 $m.s^{-1}$ during the storm, dropped towards midnight and rose again for most of the next day. This wind energy firstly ensured that the temperature in the debouchement (Fig. 5A) was homogeneous at the start of the period; secondly mixed in the heat from the daytime radiation; thirdly mixed down the colder water during the night of 1984/03/14-15; and fourthly began to mix the warmer water in

By 08:00 (e.h. 32), the current had abated sufficiently to allow temperature stratification to develop. Turbidity fell between the two peaks. As yet, the conductivity was hardly affected.

By 12:00 (e.h. 36), the second turbidity peak had begun to arrive, which probably lowered the conductivity due to aggregation. The debouchement began to stratify more strongly. Judging from temperature readings, underflow began to develop right down to Station 7.

By 16:00 (e.h. 40), the debouchement was strongly stratified due to radiation at the surface and underflow, which was by now

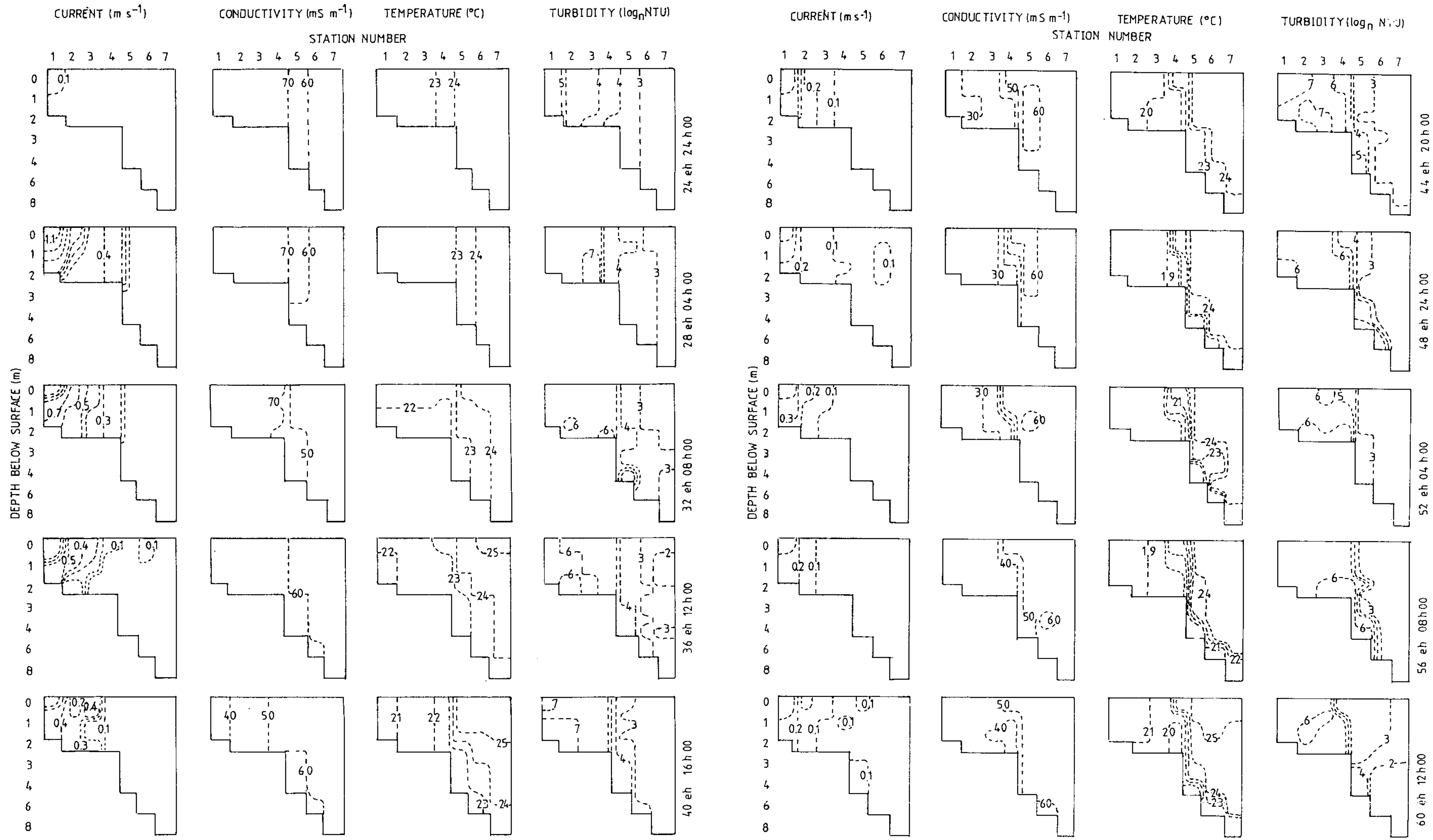

Figure 6

Contours of current, conductivity, temperature and turbidity at Stations 1 to 7 (Fig. 1B) in the debouchement of the Crocodile River into Lake Hartbeespoort during the flood of 1984/03/13-15, at 13 discrete depths and 10 nominal measurement times, from 24 to 60 elapsed hours after 00:00 on 1984/03/13.

strongly developed at Stations 5 to 7. In sympathy with the drop in current, stratification had spread to Station 4. The beginning of the second turbidity peak reached Station 2 and conductivity fell in sympathy.

At 20:00 (e.h. 44), low conductivity inflow had advanced further into the lake. The debouchement continued to be strongly stratified from Station 4 onwards. The second turbidity pulse (Fig. 3B) reached its peak. At Stations 2 to 4, turbidities tended to increase towards the bottom; currents tended either to increase or to remain constant, and temperatures increased towards the bottom at Station 3, in defiance of conventional stability. Since the most marked temperature and turbidity indications could not be attributed to analog errors in measurement and since all the trends were persistent, it is strongly suggested that a density current existed, associated with turbidity (Chikita, 1989). Since however, as stated above, firstly no analysis had been done on particle sizes, and secondly recording errors are possible when readings are taken from a boat in the dark, these observations are regarded as pointers to further research. At midnight between 1984/03/14 and 15 (e.h. 48), the second turbidity peak had begun to pass but conductivity remained low, indicating that the silt had begun to settle. It is possible that, by this stage, aggregation had stopped due to saturation. Inflow temperature reached its minimum and stratification returned to normal, apart from two possible small anomalies in the current profiles.

By 04:00 (e.h. 52), the turbidity had fallen further and conductivity began to rise. Temperature remained low. No physical explanation has been found for the anomaly in the temperature profile at Station 6. In the darkness, a recording error may therefore well have occurred.

At 08:00 (e.h. 56), the turbidity and conductivity remained constant and the inflow began to warm up, consistent with exposure to radiation during the previous day during the longer period associated with the reduced depth of the river and possibly delays in the in-line dams.

By 12:00 (e.h. 60), the inflow temperature had further increased and evidence of strong heating due to radiation appeared. In the presence of a small reduction in turbidity, conductivity began to rise. As stated above, at this stage, the two parameters may have been independent. The anomalies in the current profile may be associated with the rising wind (Fig. 5B).

Thus the entry of this isolated pulse of flood water into the lake is consistent with the properties of its previously-described origin in the catchment. Specifically, the mechanism of underflow is classical, the effect of aggregation of solutes onto particles is confirmed and there is some evidence of density currents. While errors may have occurred in certain hand readings due to the motion of the boat in darkness, and in interpretation due to variations from nominal times and interpolation of missing readings, sufficient confirmed readings and correlations to known effects and processes exist to establish the general mechanisms.

Acknowledgements

The investigation was planned, the hand measurements made and much of the analysis done at the National Institute for Water Research, now part of Environmentek, CSIR, as part of the multi-disciplinary investigation into the limnology of Lake Hartbeespoort carried out under the leadership of Dr FMChutter. The hand measurements were made by a team under the leadership of Dr J Thornton. Part of the financial backing was provided by the Foundation for Research and Development. The analysis was completed at the University of Port Elizabeth.

References

AKIYAMA J and STEFAN H (1984) Plunging flow into a reservoir: Theory. *J. of Hydraul. Eng.* **110**(4) 484-499.

ALEXANDER WJR (1990) *Flood Hydrology for Southern Africa.* The South African National Committee on Large Dams, PO Box 3404, Pretoria, 0001, RSA.

ALEXANDER WJR (undated) Flood Frequency Estimation Techniques. Course in Hydrology. Dept of Civil Engineering. University of Pretoria. Brooklyn, Pretoria 0081, RSA.

BARICA J and MUIR LR (eds) (1980) Hypertrophic ecosystems. *Dev. in Hydrol. 2.* Junk.

BOSMAN HH (1983) Spectral differences in glass and perspex thermopile shields and the effects of solar radiation measurements. *Agric. Meteorol.* **28** 65-74.

CARMICHAEL WW (1981) *The Water Environment - Algal Toxins and Health.* Plenum, New York.

CHAPRA SC (1980) Great Lakes Environmental Research Laboratory, National Oceanic and Atmospheric Administration, Ann Arbor, Michigan. Application of phosphorus loading models to river-run lakes and other incompletely mixed systems. International Symposium on Inland Waters and Lake Restoration, Portland, Maine. *EPA Report No 1;* **440**/5-81-010.

CHIKITA K (1989) A field study on turbidity currents initiated from spring runoffs. *Water Resour. Res.* **25**(2) 257-271.

CHOW VT (ed.) (1964) *Handbook of Applied Hydrology.* McGraw-Hill.

CHRISTIAN G and PARSONS WJ (1959) Semi-arid regions. In: Wisler CO and Brater EF (eds). *Hydrology.* John Wiley & Sons 286-300.

FISCHER HB, LIST EJ, KOH RCV and BROOKS NH (1979) *Mixing in Inland and Coastal Waters.* Academic. 483 pp.

FOROUD N, BROUGHTON R and AUSTIN G (1984) The effects of moving rainstorms on direct runoff properties. *Water Res. Bull.* **20**(1) 87-91.

GOTTSCHALK LC (1964) Reservoir sedimentation. In: Chow VT (ed.) *Handbook of Hydrology.* McGraw-Hill.

GROBLER DC, DAVIES E and YOUNG L (1981) The stability of sediment/water suspensions as a function of water chemistry. In: Water Year + 10 and Then? Department of Water Affairs Technical Report TR 114, P O Bag X 313, Pretoria 0001, R S A.

GROBLER DC, TOERIEN DF and ROSSOUW JN (1987) A review of sediment/water quality interaction with particular reference to the Vaal River system. *Water SA* **13**(1) 15-22.

HACH (undated) *Turbidity Measurement.* POBox 389, Colorado, 80539, USA.

HEBBERT B, IMBERGER J, LOH I and PATTERSON J (1979) Collie river underflow into the Wellington reservoir. *Proc. of the Am. Soc. of Civil Eng..* **105** 533-545.

HELD G (1988) Radar observations of thunderstorms which caused a flood in the Crocodile river. *Floods in Perspective.* Publication **C104**. South African Institution of Civil Engineers, POBox 61019, Marshalltown, RSA.

HUNTER JS (1968) *Design of Experiments Course.* Westinghouse Electric Corporation, USA.

HUTCHINSON GE (1957) *A Treatise on Limnology 1.* J Wiley & Sons, NY, 1015 pp.

IMBERGER J (1982) Reservoir dynamics modelling. Department of Civil Engineering, University of Western Australia. 57 pp.

IMBERGER J and PATTERSON JC (1990). Physical limnology. *Adv. in Appl. Mech.* **27** Academic. 303-475.

KEURIS H (1985) Personal communication. Department of Water Affairs and Forestry, Private Bag X313, Pretoria, 0001, RSA.

KOVACS ZPSJ (1978) Documentation of the January 1978 Floods in Pretoria and in the CrocodileRiver Catchment. Department of Water Affairs Report no TR 88. Private Bag X313 Pretoria 0001. 58 pp.

LINSLEY RK, KOHLER MA and PAULUS JLH (1949) *Applied Hydrology.* McGraw-Hill. 689 pp.

MACMAHON TA (1979) Hydrological characteristics of arid zones. *Proc. of the Canberra Symp., December 1979.* IAHS-AISH (International Association of Hydrological Scientists) Publ no **128**.

MEINZER OE (1942) Hydrology. *Physics of the Earth no IX,* McGraw Hill. 712 pp.

MIMIKOU MA and BALTAS EA (1996) Flood forecasting based on radar rainfall measurements. *J. Water Resourc. Man.* **122** (3) ASCE 151-156.

NATIONAL INSTITUTE for WATER RESEARCH (1985) The Limnology of Hartbeespoort Dam. SANSP Report no 110. Foundation for Research and Development, CSIR, PO Box 395, Pretoria 0001. 269 pp.

PITMAN WV (1986) Hydrology of the Hartbeespoort Dam Catchment. BKS WRA Report no. 4161/14; DWA Report no. P C00/00/5486. Department of Water Affairs and Forestry, Private Bag X 313, Pretoria 0001. R.S.A.

PITMAN WV and BASSON MS (1979) Flood Forecasting for Reservoir Operation. Report No. 1/79. Hydrological Research Unit, Department of Civil Engineering, University of the Witwatersrand, 1 Jan Smuts Avenue, Johannesburg, 2001.

PRESTON-WHYTE RA and TYSON PD (1988) *The Atmosphere and Weather of Southern Africa*. Oxford University Press, Cape Town. 365 pp.

ROBARTS RD ASHTON PJ, THORNTON JA, TAUSSIG JH and SEPHTON LM (1982) Overturn in a hypertrophic, warm, monomictic impoundment (Hartbeespoort Dam, South Africa). *Hydrobiol.* **97** 209-224.

ROOSEBOOM A (undated) Sediment transport. Hydrology course. University of Pretoria, Department of Civil Engineering, Pretoria 0181, RSA.

SMITH IR (1975) *Turbulence in Lakes and Rivers.* Freshwater Biological Association, The Ferry House, Ambleside, Cumbria, LA22 oLP, UK. 79 pp.

SMITH SH (undated, latest listed reference dated 1958). Temperature correction in conductivity measurements. Unknown Textbook. US Bureau of Commercial Fisheries, Ann Arbour, Michigan. 330-334.

STANDARD METHODS (1975) *Standard Methods for the Examination of Water and Wastewater* (14th edn.), American Public Health Association, Washington, DC.

STUMM W and MORGAN J (1970) *Aquatic Chemistry.* J Wiley, New York.

TARA MJ, GREENBERG AE, HOAK RD and RAND MC (1971) *Standard Methods for the Examination of Water and Waste-water* (13th edn.). American Public Health Association. 1015 18th st, Washington D C 20036 USA.

VAN RIET WF (1987) Hartbeespoort Dam - A magnet to millions? In: Thornton JA and Walmsley RD (eds.) Occasional Report no. **25**, Foundation for Research and Development, CSIR, PO Box 395, Pretoria 0001.

VINER A (1984) Use of the electronic particle counter to investigate phosphorus on particles in streams. *Hydrobiol.* **118** 231-236.

WARD JV (1985) Thermal characteristics of running waters. *Hydrobiol.* **125** 31-46.

WEATHER BUREAU (1987) Meteorologial Observations and Instruments. Department of Environment Affairs, Private Bag X741, Pretoria 0001.

WOODARD FE, FITCH JH and FONTAINE RA (1981) *Modelling Heavy Metal Transport in River Systems.* Land and Water Resources Centre, University of Maine at Orono.